Signals of ecological decline and increasing genomic inbreeding in Western Hudson Bay polar bears

L. Ruth Rivkin, Evan S. Richardson, Samuel Deakin, David McGeachy, Joshua M. Miller, Colin J. Garroway

Affiliations

Ruth Rivkin: Department of Biological Sciences, University of Manitoba, Winnipeg, MB, Canada; Polar Bears International, Bozeman, MT, USA

Evan Richardson: Environment and Climate Change Canada, Biodiversity Research Division Winnipeg, MB, Canada

Samuel Deakin: Department of Biological Sciences, University of Alberta, Edmonton, AB, Canada

David McGeachy: Environment and Climate Change Canada, Biodiversity Research Division, Edmonton, AB, Canada

Joshua Miller: Department of Biological Sciences, MacEwan University, Edmonton, AB, Canada

Colin Garroway: Department of Biological Sciences, University of Manitoba, Winnipeg, MB, Canada

Email for correspondence: ruth.rivkin@umanitoba.ca

Abstract

Climate change is a leading cause of population declines. Predicting the evolutionary consequences of such declines can be challenging for long-lived species because slow generation times and the overlap of individuals from multiple generations within a population can obscure signals of genetic diversity losses. We integrated four decades of environmental, demographic, and genomic data from the Western Hudson Bay polar bear subpopulation to assess whether genomic signatures of inbreeding have accumulated during a well-characterized period of climate-mediated habitat loss. This subpopulation occurs at the species' southern range edge, where the consequences of climate change are particularly acute. Against the background of declining sea ice availability and population abundance, genomic inbreeding increased in 533 polar bears sampled from progressively later birth cohorts. The increase was concentrated in runs of homozygosity, whose lengths indicate shared ancestry approximately 3–16 generations ago. This interval overlaps with unregulated polar bear harvest in the 1900s, suggesting a legacy of historical overharvesting. While the signal of increasing inbreeding raises questions about then potential of evolutionary decline in the subpopulation, very recent inbreeding was rare, suggesting that the expression of inbreeding depression may be offset by extensive gene flow in the species.

Keywords: Arctic, demographics, inbreeding rate, management, Runs of Homozygosity, sea ice, *Ursus maritimus*

Background

Climate change and habitat loss are key contributors to declines in population abundances, range contractions, and extirpations [1,2]. As many as 32% of vertebrate species have experienced some degree of population decline within the last 125 years [3], and declines are predicted to scale with the degree of habitat specialization [4]. Population declines are often associated with negative evolutionary outcomes as shrinking populations become more prone to inbreeding, experience greater erosion of genetic variation, and ultimately exhibit decreased capacity for adaptation [5,6]. However, the rate of genetic decline may be slower in species with long lifespans, slow generation times, and complex mating structures [7], potentially masking the evolutionary consequences of population declines. Here, we use four decades of environmental and demographic monitoring in the Western Hudson Bay polar bear (*Ursus maritimus*) subpopulation to ask whether genomic signatures of inbreeding have accumulated during a well-characterized, climate-driven population decline.

Polar bears are among the most-studied wildlife species in the Arctic [8] and provide an opportunity to examine the relationship between demographic and genomic decline within the context of climate change-driven habitat loss. Polar bears span the circumpolar Arctic, where they have been grouped into 20 subpopulations for management purposes (Figure S1; IUCN/SSC Polar Bear Specialist Group 2024). Polar bears are adapted to sea ice, relying on it for hunting, dispersal, and mating; the species has experienced significant habitat loss due to climate warming [10]. Rapid warming associated with climate change has increased the length of the ice-free season, during which polar bears fast while on land [11,12]. Extended fasting periods are associated with reduced reproductive success, lower survival rates, and in some subpopulations, declines in abundance (e.g., [13–16]).

Long-term monitoring of the Western Hudson Bay subpopulation (Figure S1) has provided some of the strongest evidence of polar bear population decline associated with sea ice loss [15]. The Western Hudson Bay subpopulation is the site of the longest-running polar bear monitoring program, dating back to the 1960s [17]. Several studies have identified persistent signals of population decline concurrent with sea ice loss in the subpopulation [15,18]. Although widely believed to be a subpopulation in decline, differences in survey approach and duration have inhibited long-term assessments of the rate of decline, and it is unknown if such declines have led to evolutionary change in the subpopulation.

We assessed associations between ecological and evolutionary signals of population decline in the Western Hudson Bay subpopulation by integrating environmental data, previously published demographic data (Table S1), and genomic data from tissue samples collected over 40 years of continuous monitoring. We asked how changes in habitat availability and population abundance during this period may have shaped genomic inbreeding rates through time. We inferred genomic signatures of inbreeding from the accumulation of autozygosity measured by Runs of Homozygosity (ROH) across the genome. ROHs are contiguous genomic regions composed of identical haplotypes inherited from a shared ancestor. Genomic inbreeding measured from ROHs is associated with reduced fitness across taxa, with particularly strong associations with survival in wild populations [19]. ROH length also provides information about the recency of shared ancestry; longer ROHs generally reflect more recent common ancestry, whereas shorter ROHs persist from more distant ancestry and historical population processes [20,21]. Both short and long ROHs can contribute to inbreeding depression [19]. The inbreeding coefficient (F_{ROH}) measures the proportion of the genome that contains ROHs relative to the total size of the sequenced portion of the genome. We hypothesized that reduced habitat availability

and population abundances would be associated with increased autozygosity and inbreeding rates, indicative of an evolutionary decline in the subpopulation.

Methods

Sea Ice Quantification

Hudson Bay is a large, shallow inland sea that is seasonally covered by sea ice. Sea ice forms in late fall and breaks up in spring, with an ice-free period spanning 4-6 months in the summer. We quantified changes in sea ice cover in the Hudson Bay from 1979 to 2021. We obtained monthly sea ice area (km^2) and extent (km^2) estimates from the National Snow and Ice Data Center Sea Ice Index [22]. The Sea Ice Index is based on the NASA-produced Sea Ice Concentrations from Nimbus-7 SMMR and DMSP SSM/I Passive Microwave Data (https://nsidc.org/data/nsidc-0051) and AMSR2 Daily Polar Gridded Sea Ice Concentrations (https://nsidc.org/data/nsidc-0803/versions/1), at a spatial resolution of 25 km x 25 km. Sea ice area is the sum of the grid cell areas weighted by their ice concentration for cells with ≥15% concentration, whereas extent is the total area of grid cells with ≥15% ice concentration [22].

We downloaded the North Regional Sea Ice Monthly dataset, which provides monthly estimates for the Hudson Bay. The area captured in the dataset encompasses the entirety of Hudson Bay, including regions that fall outside the Western Hudson Bay subpopulation boundaries, such as Foxe Basin, James Bay, and the Hudson Strait [23]. We averaged the monthly values to obtain a single mean estimate of area and extent per year from 1979-2021. This timeframe corresponded to the sampling period covered by the previously published polar population abundance estimates for the region (Table S1).

Abundance Estimates

The Western Hudson Bay subpopulation is the site of a long-term research program dating back to 1966 [17,24]. Each year, Environment and Climate Change Canada captures, marks, and releases a random sample of polar bears from the Western Hudson Bay subpopulation. Data on abundance, population recruitment, body condition, and body size are collected, along with physical samples of skin, fat, blood, and other specimens [17]. During capture, bears are chemically immobilized using standard techniques [25]. Birth year is determined for dependent bears (≤2 years old and still with their mothers) using morphometrics and tooth eruption patterns, while independent bears are aged via cementum annuli in extracted teeth [26]. All animal handling follows approved protocols from Environment and Climate Change Canada's Western and Northern Animal Care Committee, under wildlife research permits issued by the Province of Manitoba and Parks Canada. Abundance estimates derived from mark-recapture data provided the first population estimates for the subpopulation [18,27,28], with subsequent analyses using both live captures and dead recoveries from harvest [15], or more recently, aerial surveys (Table S1).

We used a meta-analytic approach to assess temporal change in abundance in the Western Hudson Bay subpopulation (see *Bayesian Regression Modelling* below). We identified seven studies that reported annual estimates in abundance in the subpopulation spanning 1979-2021 (Table S1). These studies differed in their survey techniques (e.g., capture-recapture versus aerial surveys) and modelling approaches to derive annual abundance point estimates and their associated error estimates. Although other studies (e.g., [32,33]) have reported abundance estimates for the subpopulation, these were derived by re-analysing existing data with updated models rather than from new survey data, and we excluded them from our meta-analysis to avoid pseudoreplication. We also excluded abundance estimates derived for 1985-1986 from Lunn et

al. [15] and Regehr et al. [18], as per the authors' recommendations, because incomplete sampling of the core summering areas produced negatively biased abundance estimates that were not considered comparable with estimates from subsequent years.

We extracted point estimates and error intervals directly from the text for three studies [29–31]. For the remaining four studies, we extracted point estimates and error intervals using WebPlotDigitizer v5.2 [34], an accurate, web-based plot digitizing tool for extracting data from figures [35]. Four studies reported error terms as 95% confidence/credible intervals, and we manually converted these estimates to approximately normal standard error terms ($Standard\ Error \sim \frac{\text{Upper interval} - \text{Lower interval}}{2*1.96}$) to facilitate comparisons among studies.

Sample Collection

We sequenced 561 polar bears sampled between 1982 and 2018 as part of the long-term monitoring program in the Western Hudson Bay subpopulation. We included approximately equal numbers of males and females (51% female). We primarily selected bears (92% of samples) with low apparent fitness to improve our ability to detect signals of inbreeding depression by including bears that were not recaptured by the monitoring program. These bears were observed only as cubs of the year (< 1 year old), so we presume they did not survive to maturity or produce offspring. Mortality of young polar bears is high in Western Hudson Bay, with a first-year survival of ~50% [36–38], and age of first reproduction is between 5 and 7 years old for females and 9 and 10 years old for males [36,39]. Bears that have not been recaptured are typically not included in other sample designs for the subpopulation [40,41]; thus, patterns of genetic variation have not been fully explored in this group. Given that survival is among the fitness traits most strongly associated with genomic inbreeding in wild populations [19],

enriching our sample for bears that likely died young was intended to improve our ability to detect genomic signatures of inbreeding associated with low fitness. We also sampled bears that were subsequently recaptured (N = 42), allowing us to account for recapture status when assessing temporal patterns of genomic inbreeding.

Probe Design and Sequencing

We developed a high-density targeted SNP assay to detect signatures of inbreeding in polar bears. We sequenced the DNA using Allegro Targeted Genotyping from Tecan Genomics (Redwood City, CA, USA), a form of genotype-by-sequencing that targets pre-selected loci for amplification and probe development. This method uses Single Primer Enrichment Technology to amplify genomic regions surrounding each probe site, generating 80-120 bp fragments that include the probe and adjacent downstream genomic regions [42]. We developed probes using markers present on the *Ursus maritimus V1* and *V2* SNP chips [40,41]. We used a combination of variable restriction-site associated DNA (RAD)-loci, Sanger loci, and transcriptomic loci that appear on both chips, as well as 44 additional loci that appear on the Y chromosome. In total, we submitted 4,907 loci to Tecan Genomics (Redwood City, CA, USA) for target development, which resulted in a final dataset of 4,801 probes.

DNA was extracted from polar bear skin and muscle with Qiagen DNeasy Blood & Tissue kits (Qiagen, Hilden, Germany). We prepared libraries, including eight replicate samples, using Allegro Targeted Genotyping V1 kit following the manufacturer guidelines with the fragmentation digest time increased to 22.5 min. We sequenced the libraries on an Illumina NextSeq using the NextSeq V2.5 mid-output 300 cycle kit (San Diego, CA, USA), generating 150 bp paired-end reads.

Variant Calling and Filtering

We filtered low-quality reads using TrimGalore! v0.6.6, a wrapper program for Cutadapt v1.14 [43]. We retained reads with a Phred score greater than 20 and a minimum read length greater than 30. Following manufacturer guidelines, we trimmed the 40 basepair (bp) probe derived sequences from the 5' end of the forward read and the 15 bp probe linker and adapter sequences from the 3' end of the reverse read. We mapped reads to the UrsMar_1.0 reference genome (GCA_000687225.1) with BWA v0.7.18-r1234-dirty [44]. We soft-clipped probe sequence reads to prevent them from being called downstream and aligned and sorted reads with samtools v1.13 [45].

We used bcftools v1.21 [45] to call variants in two steps. First, we called variants captured directly within the probe regions. We called variants a second time in genomic regions that fall adjacent to, but outside of, the probe regions. This strategy allowed us to identify variants along longer stretches of the genome and is better suited to identifying ROHs. We used bcftools to remove variants with low-quality scores, strand bias, read mismatch, and multi-allelic calls, as well as those with depth < 10x and genotype quality < 20. We concatenated the probe and flanking variant files, allowing overlaps, and filtered the final dataset to include variants and samples with >90% call rates. Lastly, we selected the 99 scaffolds with the greatest number of SNPs to meet the program requirements for detecting ROHs [46]. The remaining scaffolds covered 1.5 GB (65%) of the genome.

Genomic Signatures of Inbreeding

We used PLINK v1.9 [47] to identify ROHs in sliding windows across the genome. We selected parameters to remove very short ROHs that have arisen due to founder effects from the

relatively recent speciation of polar bears [48]. To avoid accidentally removing long ROHs, we did not filter our input files for linkage disequilibrium or minor allele frequency [49]. We selected ROHs that were at least 300 Kb long (homozyg-kb) and with no more than 1000 Kb between consecutive SNPs (--homozyg-gap). We included a maximum of one heterozygous call per ROH (--homozyg-het) and five per window (--homozyg-window-het).

We estimated the minimum number of SNPs needed to avoid including artificially small ROHs [50,51]. We calculated the *l*-parameter ($l = \frac{log_e(\frac{\alpha}{n_s \cdot n_i})}{log_e(1-\overline{het})}$), where α is the percentage of false positive ROHs (set to 0.05), n_s is the number of SNPs per individual, n_i is the number of individuals in the study, and $\overline{het}$ is the mean heterozygosity across all SNPs [51]. We calculated mean heterozygosity using PLINK, after filtering the SNP dataset for Hardy-Weinberg equilibrium and minor allele frequency. The *l*-parameter estimate we generated was 54, which is in line with the estimate generated by for polar bears (l = 61; [50]). We assigned this value to the minimum number of SNPs per ROH (--homozyg-snp) and per window (--homozyg-window-snp). All other parameters were set to default.

We used detectRUNS v0.9.6.9004 [46] to summarize the length of ROHs observed per window. We classified ROHs as short (< 1Mb), long (1-5 Mb), and very long (> 5 Mb). We calculated individual F_{ROH} for each of these classes as: $F_{ROH} = \frac{\sum L_{ROH}}{L_{genome}}$, where ΣL_{ROH} is the sum of the length of ROHs that fall within the size class per individual, and L_{genome} is the total length of the genome that was captured by sequencing. We estimated the timing of inbreeding as: $g = \frac{100}{2rL}$, where g is the number of generations since inbreeding, r the recombination rate, and L is the length of ROH in Mb [52]. We used a recombination rate of 3.1 cM/MB (D. Desai and A.

Schafer, personal communication) and a generation time of 11.5 years to convert generations into years [53].

Bayesian Regression Modelling

We assessed the change in sea ice, abundance, and inbreeding with Bayesian regression modeling using the R package brms v2.23.0 [54]. All models were performed with 4 Markov chains, 10,000 iterations, and 3,000 warmup iterations, and were fit to Gaussian distributions unless otherwise stated. Where necessary, we increased the tree depth and model acceptance rate to improve convergence. For all models, we evaluated the suitability of the priors by visually inspecting their distributions and performing prior predictive checks to compare the observed data with predictions.

We modelled the change in sea ice area and extent with year (1979-2021). We assigned a weakly informative prior to year following a Student's t-distribution with a mean of 0, a standard deviation of 2.5, and 1 degree of freedom.

We modelled the change in abundance over years (1979-2021) using a hierarchical meta-analytical model structure to account for uncertainty in estimates within studies and variation between studies [55]. We accounted for variation in the precision of estimates within studies by weighting the point estimates of abundance by their standard error and allowing the model to estimate residual standard error. We quantified variation between studies by assigning random slopes and intercepts to each study. We assigned loosely informative priors to year, following a Student's t-distribution with a mean of 0, a standard deviation of 2.5, and 1 degree of freedom, and to the correlation between random effects following a Cholesky Lewandowski-Kurowicka-Joe (LKJ) distribution with equal likelihood across all correlations.

We developed three additional models to assess the impact of repeated measures, non-linear distribution, and potential outliers. We assessed the impact of repeated measures on the same population by truncating the dataset to include only the most recent estimate per year (N = 38 data points) and repeating the analysis. We also modelled a non-linear relationship between abundance and time to determine whether population size may have increased prior to the decline. We added a quadratic term for sampling year to the abundance model, with year standardized by its mean and standard deviation to reduce collinearity between terms. We compared the fit of the linear and quadratic models using a leave-one-out cross-validation analysis [56]. Lastly, we assessed the effect of excluding the estimates from Atkinson et al. [31], who identified a 27% decline in abundance in 2021 in the subpopulation, which is likely the result of a temporary emigration to a neighbouring subpopulation [31,57].

Finally, we modelled the change in genomic inbreeding and ROH buildup using polar bear birth year as a proxy for time (1968-2018). We included three models in this group. The first two models assessed changes in inbreeding associated with short ($F_{ROH} < 1$ Mb) and long ($F_{ROH} =$ 1-5 Mb) ROHs through time. We did not include $F_{ROH} > 5$ Mb because there were too few very long ROHs to achieve an adequate model fit. Instead, the third model assessed changes in the number of very long ROHs (> 5 Mb) over time using a zero-inflated Poisson distribution. We statistically controlled for the effects of presumed survival on inbreeding by including recapture as a fixed effect in each model. For all three models, we assigned weakly informative priors to birth year following a Student's t-distribution with a mean of 0, a standard deviation of 2.5, and 1 degree of freedom, and a normal distribution with mean 0 and standard deviation 1 to recapture.

We quantified directional support for each temporal trend using posterior probabilities, calculating the posterior probability that slopes were less than zero for sea ice and abundance and

greater than zero for F_{ROH} and ROH counts. We considered posterior probabilities >95% strong support for the predicted direction of an effect. Lastly, we visualized changes in sea ice availability, abundance, and genomic inbreeding over time by plotting the posterior mean distributions. For each plot, we calculated 50%, 80%, and 95% credible intervals by sampling from the posterior predictive distribution of the models to visualize uncertainty.

Results

We identified a consistent signal of habitat loss in the Hudson Bay. The Bayesian regression models predicted a decline in sea ice coverage through time (Table 1). Sea ice area declined at a rate of 2,256 km^2 per year (Posterior Probability >95%, Figure 1A), while extent declined at a 2,624 km^2 per year (Posterior Probability >95%, Figure S2).

The Bayesian meta-analysis model predicted a linear decline in abundance through time (Table 1). Although the magnitude and slopes of the trends varied among studies (Figure S3), on average across studies, abundance declined at a rate of 10.9 polar bears per year (Posterior Probability >95%, Figure 1B). Adding a quadratic term did not materially improve predictive performance relative to the linear model (ΔELPD = −1.9, SE = 1.0; Figure S4). There was no effect of truncating the dataset or of dropping data from Atkinson et al. [31] on model outcomes (rate of decline: 10.5 bears per year; Posterior Probability >95%, Figure S5).

The SNP dataset contained 43,262 SNPs with a call rate of 93% from 533 individuals. The average observed heterozygosity across all individuals was 0.23. We identified 101,968 ROHs ranging in length from 301 kb to 12.2 Mb. Most ROHs (75%) were between 1-5 Mb, while short ROHs (<1 Mb) formed 26% of the dataset, and very long ROHs (>5 Mb) formed

0.5% of the dataset (Figure 1C). Bears that were recaptured had an average of 190 ROHs, while bears that were not recaptured, and presumably did not survive, had an average of 187 ROHs.

Average F_{ROH} across all size classes was 0.20 and did not differ based on recapture. F_{ROH} was predominantly contributed by ROHs of 1-5 Mb (mean F_{ROH} < 1 Mb = 0.02, 1-5 Mb = 0.17, and > 5 Mb = 0.01). For 1–5 Mb ROHs, the expected time to shared ancestry was approximately 3.2–16.1 generations, or 37–185 years before each bear's birth, assuming a generation time of 11.5 years.

The Bayesian regression models predicted an increase in inbreeding associated with long ROHs as birth year increased (1968-2018). F_{ROH} = 1-5 Mb increased with birth year (Posterior Probability >95%, Table 1, Figure 1D). Evidence for temporal change in FROH < 1 Mb was weaker (Posterior Probability = 79%; Table 1, Figure S6), indicating that the increase in genomic inbreeding was concentrated in the 1–5 Mb ROH class. Evidence for an increase in the number of very long ROHs (>5 Mb) was also weak (Posterior Probability = 62%; Table 1, Figure S7). There was no effect of recapture in any of the models (Table 1).

Discussion

We found consistent evidence of correlated evolutionary and ecological decline in the Western Hudson Bay polar bear subpopulation. We identified an increase in genomic inbreeding driven by long ROHs (1-5 Mb) across the 40-year monitoring period. ROHs of this length reflect relatively recent shared ancestry. Using the Western Hudson Bay-derived recombination rate of 3.1 cM/Mb, 1–5 Mb ROHs correspond approximately to shared ancestry 3–16 generations, or 37–185 years before each bear's birth. This period overlaps with unregulated harvest of polar bears during the 1900s, suggesting that historical harvest pressure may have contributed to the

306 autozygosity observed today [58]. In 1973, the five circumpolar range nations signed the
307 Agreement on the Conservation of Polar Bears to restrict polar bear harvesting to traditional
308 Indigenous rights [59]. Despite the reduction in harvest pressure, increasing genomic inbreeding
309 within the subpopulation suggests an ongoing evolutionary decline that may eventually lead to
310 an erosion of genetic variation and reduced capacity for adaptive responses to warming [12].
311 However, given the relatively slow buildup of autozygosity in the subpopulation, other
312 evolutionary forces such as gene flow could buffer the loss of genetic variation associated with
313 increased inbreeding.

314 Interestingly, very long ROHs (>5 Mb) were rare in the subpopulation, suggesting that
315 inbreeding depression associated with very recent inbreeding (within 1–3 generations) may be
316 limited. Bears recaptured after their first year had a slightly higher number of very long ROHs,
317 suggesting that presumed survival was not lower among bears with very long ROHs. However,
318 recaptured bears formed a small proportion of samples, which may have reduced our power to
319 detect differences between groups. We also cannot rule out that the rarity of very long ROHs
320 may be an artifact of our sequencing method. Reduced-representation sequencing approaches are
321 more affordable than whole genome sequencing but result in lower coverage and marker density
322 which may hinder the detection of very long ROHs due to fragmentation of these genomic
323 stretches during sequencing [20]. Reassessment of very long ROHs using whole-genome data
324 and a different sample set would provide a stronger test of inbreeding depression in the
325 population.

326 The genomic and pedigree-based inbreeding rates of the subpopulation differed
327 dramatically. The pedigree-based inbreeding rate of the subpopulation is less than 1% [60]. This
328 estimate was generated by calculating the inbreeding coefficient among close relatives

329 (offspring, parents, and grandparents). In contrast, genomic estimates of inbreeding can detect
330 subtle shifts in inbreeding rates between more distantly related individuals, particularly under
331 instances of incomplete pedigree resolution [61,62]. In wild populations, pedigree-based
332 estimates of inbreeding consistently underestimate inbreeding relative to marker-based estimates
333 [63–65]. The ability of genetic markers to accurately detect inbreeding rates provides
334 opportunities to enhance the effective conservation of wild populations, which frequently lack
335 pedigree information [66].

336 We identified higher rates of inbreeding than previous F_{ROH} estimates for polar bears [50].
337 This discrepancy may be best explained by sampling differences between studies. We sampled
338 more than 500 bears from a small, southerly region of the range that has experienced large
339 reductions in sea ice availability, and we selected primarily for individuals with low fitness. In
340 contrast, Clendenin et al. [50] included 25 polar bears sampled from the species' northern
341 circumpolar range. Sea ice conditions have shifted towards a seasonal sea ice environment in the
342 High Arctic, but polar bear subpopulations in this region have not experienced the same declines
343 in body condition or population size as polar bears in more southern regions [67,68].
344 Consequently, we may have detected an early signal of evolutionary decline in the species in
345 response to climate warming. Given projected sea ice loss over the next century [69], we
346 anticipate similar declines throughout the polar bear range.

347 Between 1979 and 2021, our models support the hypothesis that habitat availability and
348 population abundance estimates declined, coinciding with increased inbreeding rates in the
349 population. Sea ice loss is well documented in the Arctic [70,71], and has been linked to reduced
350 viability in several polar bear subpopulations, including the Western Hudson Bay (e.g., [13–
351 15,72,73]). The ice-free period in Hudson Bay, including Foxe Basin and the Hudson Strait, has

lengthened by approximately one month [74,75], although some models support a step change in the date of sea ice breakup in 1989, with little change afterward [76]. Within the Western Hudson Bay subpopulation, several studies support an increase of approximately 10 ice-free days/decade [16,32,77]. During the ice-free period, polar bears are restricted to land and typically fast until sea ice forms again. Despite foraging opportunistically at whale carcasses and other food sources, most bears lose 1 kg of body mass per day while onshore [78–80]. Physiological constraints on fasting duration are stronger for lactating females and young bears [81], and years with earlier ice breakup are associated with lower survival rates in these groups [15].

Accordingly, the decline in abundance in the Western Hudson Bay has been attributed primarily to lower survival rates among females, cubs, and subadult bears [15,18,31]. Initial reports for the subpopulation indicated a stable or increasing population from 1979-1990, likely due to rebound effects following the 1973 ban on commercial harvest [27,28]. A period of rapid decline was reported from the 1990s to the mid-2000s associated with rapid sea ice loss in the region, followed by relative population stability [15,18,30]. The most recent aerial survey estimate identified a 27% drop in abundance between 2016 and 2021, with an approximately equivalent increase in abundance in the neighbouring Southern Hudson Bay subpopulation [31,82]. Biopsy sampling across both subpopulations during the same period supports the hypothesis that the decline is the result of the movement of bears between adjacent subpopulations rather than a reflection of poor survival outcomes [57,83]. However, we identified a sustained decline in abundance that persisted even after the final 2021 estimate was excluded, and we did not we find evidence of a quadratic relationship between abundance and time, suggesting that, despite recent periods of relative stability, the compiled abundance estimates support a long-term decline across the 40-year monitoring period.

The variation in trends observed among studies is likely due to annual variation in sea ice conditions but may also reflect differences in survey methods. Early population surveys relied on capture-recapture census methods, with a switch to aerial surveys beginning in 2011 (Table S1). Aerial surveys cover nearly the entire area of the Western Hudson Bay subpopulation, whereas capture-recapture methods typically focus on a core population area [18,29]. Direct comparisons between studies are challenging because modelling approaches and assumptions can differ substantially between methods [29,84]. We accounted for variability in the sampling approach by incorporating study ID as a random factor in our models, allowing study intercepts and slopes to vary independently. We also weighted support for individual point estimates by their standard errors, thereby reducing the influence of lower-precision estimates in the model. This conservative approach permits comparisons across studies while remaining sensitive to the individual differences among population census approaches.

Conclusions

Using genome-wide signatures of autozygosity, we identified clear evidence for recent increases in inbreeding and a persistent legacy of overharvest The increasing rate of inbreeding and long-term decline in abundance and habitat availability raise questions about the evolutionary stability of the Western Hudson Bay subpopulation. Inbreeding increases homozygosity and can expose recessive deleterious alleles, leading to declines in fitness [85]. However, we did not find an increase in very long ROHs, suggesting that the subpopulation may not yet be at risk for inbreeding depression.

Gene flow may be offsetting the onset of inbreeding depression in the subpopulation. Even modest gene flow can reduce inbreeding and help maintain genetic variation, although the amount required depends on population size, structure, and demography [86]. Despite moderate

philopatry to their summer range, in winter, polar bears migrate to the sea ice on the Hudson Bay to hunt and mate with other bears returning to the same region from other subpopulations [87,88]. As a result, gene flow between neighbouring subpopulations is high, providing opportunities for outcrossing and allowing novel, potentially beneficial alleles to be shared among subpopulations [89]. However, disruptions to winter sea ice formation from warming temperatures and shipping traffic in the Hudson Bay will likely alter existing patterns of gene flow among subpopulations. Management strategies that continue to incorporate genetic monitoring to promote connectivity throughout the Hudson Bay offer an opportunity to support the ecological and evolutionary integrity of the subpopulation.

Acknowledgements

Financial and logistical support for the long-term study of polar bears in Western Hudson was provided by Churchill Northern Studies Centre, Earth Rangers Foundation, Environment and Climate Change Canada, Isdell Family Foundation, Manitoba Sustainable Development, Natural Sciences and Engineering Research Council of Canada (NSERC), Nunavut Wildlife Research Trust Fund, Parks Canada Agency, Polar Bears International, the Strategic Technology Applications of Genomics in the Environment (STAGE) funding programme, the University of Alberta, Weston Family Foundation, Wildlife Media Inc. and the World Wildlife Fund. We are grateful for the long-term contributions of Ian Stirling, Nick Lunn, Dennis Andriashek, Andrew Derocher, Cheryl Spencer and Wendy Calvert to the Western Hudson Bay polar bear program. We thank Corey Davis for assistance with probe design. We also thank Knox Carey and Bart Grantham from Interval Bio for help with variant calling and filtering. LRR was supported by a NSERC Postdoctoral Research Fellowship and a Weston Family Fellowship in Northern Research.

Tables

Table 1. Bayesian regression model statistics for the models investigating change in sea ice, abundance, and genomic inbreeding through time. The table displays the model response variable, the name and type (fixed versus random effect) of the predictor investigated, the slope of the predictor and 95% upper and lower credible interval bounds. The table also reports the direction of the one-sided hypothesis test and the posterior probability of the test. Posterior probabilities > 0.95 are equivalent to a significant p-value in frequentist statistical models and have been bolded. For all models, effective sample sizes were > 4000 and Rhat = 1.

Model	Predictor	Type	β	Lower CI	Upper CI	Hypothesis Test	Posterior Probability
Sea Ice Area	Year	Fixed	-2256.62	-3285.70	-1074.57	$\beta < 0$	**> 0.95**
Sea Ice Extent	Year	Fixed	-2623.93	-3637.82	-1535.39	$\beta < 0$	**> 0.95**
Abundance	Year	Fixed	-10.90	-16.18	-5.53	$\beta < 0$	**> 0.95**
	Study	Random	0.05	0	0.15	-	-
F_{ROH} < 1 Mb	Birth Year	Fixed	1.59×10^{-5}	-2.24×10^{-5}	5.40×10^{-5}	$\beta > 0$	0.79
	Recaptured	Fixed	7.52×10^{-4}	-2.38×10^{-4}	1.72×10^{-3}	-	-
F_{ROH} = 1-5 Mb	Birth Year	Fixed	5.26×10^{-4}	2.70×10^{-4}	7.86×10^{-4}	$\beta > 0$	**> 0.95**
	Recaptured	Fixed	0.00430	-0.00238	0.0108	-	-
ROH > 5 Mb	Birth Year	Fixed	0.00222	-0.0120	0.0163	$\beta > 0$	0.62
	Recaptured	Fixed	0.200	-0.147	0.527	-	-

Figures

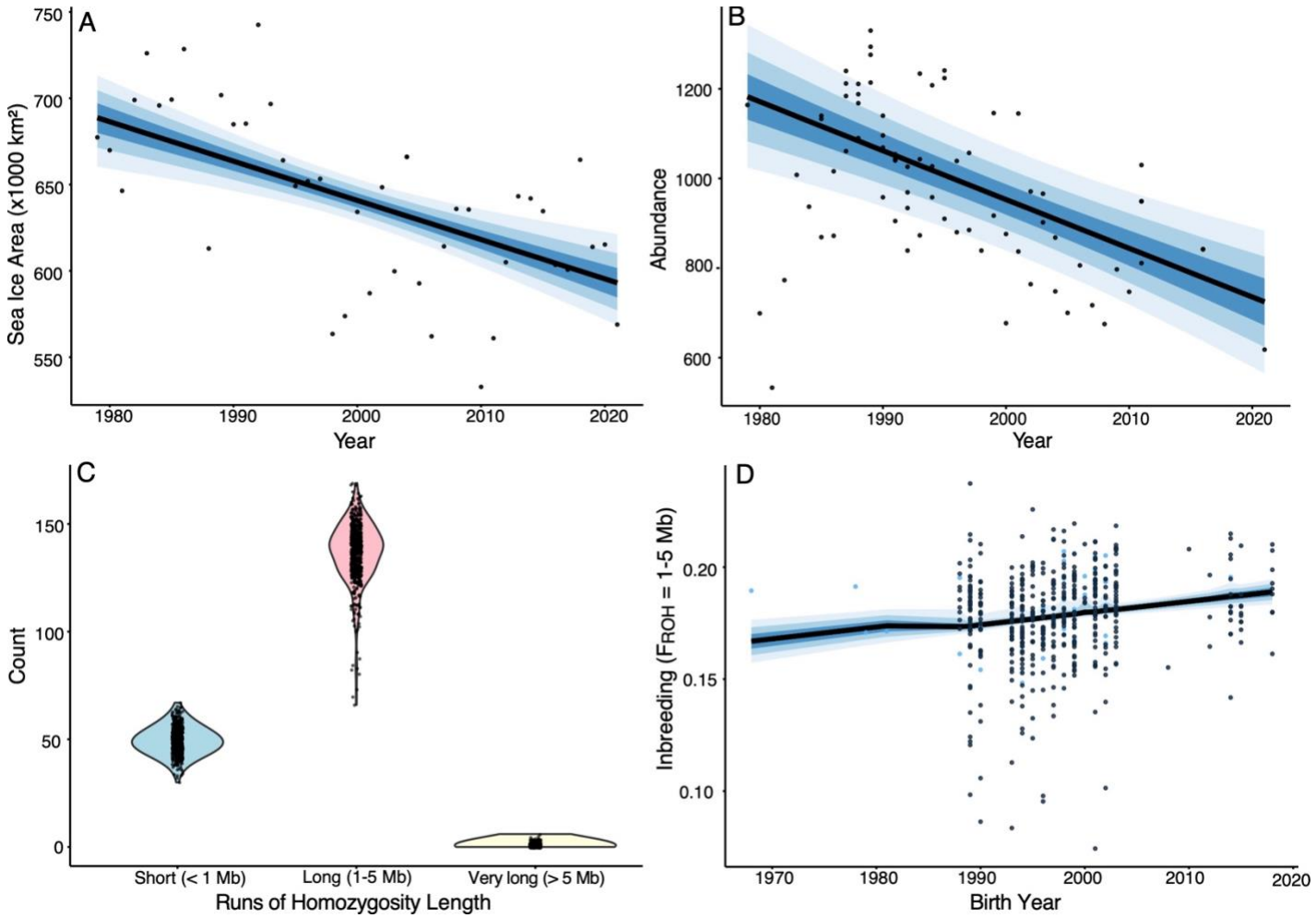

Figure 1. A) Posterior distribution of the decline in mean annual sea ice area in the Hudson Bay from 1979-2021, with 50%, 80%, and 95% credible intervals displayed. B) Posterior distribution of the change in abundance through time in the Western Hudson Bay polar bear subpopulation from 1979-2021. Each point represents an annual estimate generated from previously published studies, and credible intervals (50%, 80%, and 95%) account for within and between-study variation in estimates. C) Violin plot showing the distribution of Runs of Homozygosity size classes among 533 polar bears in the Western Hudson Bay subpopulation time. Individual data points for each size class have been superimposed over top of the plots. D) Posterior distribution, with 50%, 80%, and 95% credible intervals, of the increase in genomic inbreeding calculated from long runs of homozygosity (F_{ROH} = 1-5 Mb) with birth year (1968-2018) of polar bears as a proxy for time. Each point represents an individual bear in the analysis, and blue points denote individuals who were recaptured by the monitoring program. For A, B, and D, credible intervals where shown are presented in lightening shades of blue (50% true blue, 80% mid-blue, 95% pale blue).

Literature Cited

1. Mantyka-Pringle CS, Visconti P, Di Marco M, Martin TG, Rondinini C, Rhodes JR. 2015 Climate change modifies risk of global biodiversity loss due to land-cover change. *Biol. Conserv.* **187**, 103–111. (doi:10.1016/j.biocon.2015.04.016)

2. Habibullah MS, Din BH, Tan S-H, Zahid H. 2022 Impact of climate change on biodiversity loss: global evidence. *Environ. Sci. Pollut. Res.* **29**, 1073–1086. (doi:10.1007/s11356-021-15702-8)

3. Ceballos G, Ehrlich PR, Dirzo R. 2017 Biological annihilation via the ongoing sixth mass extinction signaled by vertebrate population losses and declines. *Proc. Natl. Acad. Sci.* **114**, E6089–E6096. (doi:10.1073/pnas.1704949114)

4. Colles A, Liow LH, Prinzing A. 2009 Are specialists at risk under environmental change? Neoecological, paleoecological and phylogenetic approaches. *Ecol. Lett.* **12**, 849–863. (doi:10.1111/j.1461-0248.2009.01336.x)

5. Kimura M, Crow JF. 1963 The measurement of effective population number. *Evolution* **17**, 279–288. (doi:10.2307/2406157)

6. Lande R, Barrowclough GF. 1987 Effective population size, genetic variation, and their use in population management. In *Viable Populations for Conservation* (ed ME Soulé), pp. 87–124. Cambridge: Cambridge University Press. (doi:10.1017/CBO9780511623400.007)

7. Kuo C-H, Janzen FJ. 2004 Genetic effects of a persistent bottleneck on a natural population of ornate box turtles (*Terrapene ornata*). *Conserv. Genet.* **5**, 425–437. (doi:10.1023/B:COGE.0000041020.54140.45)

8. Black AL, Akearok JA, Mallory ML. 2025 Long-term wildlife research and monitoring sites in Arctic Canada. *Arct. Sci.* **11**, 1–13. (doi:10.1139/as-2025-0021)

9. IUCN/SSC Polar Bear Specialist Group. 2024 Status Report on the World's Polar Bear Subpopulations. 1–60.

10. Stern HL, Laidre KL. 2016 Sea-ice indicators of polar bear habitat. *The Cryosphere* **10**, 2027–2041. (doi:10.5194/tc-10-2027-2016)

11. Stirling I, Derocher AE. 2012 Effects of climate warming on polar bears: A review of the evidence. *Glob. Change Biol.* **18**, 2694–2706. (doi:10.1111/j.1365-2486.2012.02753.x)

12. Rivkin LR, King CKC, Aars J, Laidre KL, Langwieder A, McGeachy M, Newediuk L, Petersen SD, Pilfold N, AP Wilder, *et al*. 2026 Climate-linked evolution and genetics in a warming Arctic. *Ecol. Monogr.* **96**, e70053. (doi:10.1002/ecm.70053)

13. Rode KD, Amstrup SC, Regehr EV. 2010 Reduced body size and cub recruitment in polar bears associated with sea ice decline. *Ecol. Appl.* **20**, 768–782. (doi:10.1890/08-1036.1)

14. Bromaghin JF, McDonald TL, Stirling I, Derocher AE, Richardson ES, Regehr EV, Douglas DC, Durner GM, Atwood T, *et al.* 2015 Polar bear population dynamics in the southern Beaufort Sea during a period of sea ice decline. *Ecol. Appl.* **25**, 634–651. (doi:10.1890/14-1129.1)

15. Lunn NJ, Servanty S, Regehr EV, Converse SJ, Richardson E, Stirling I. 2016 Demography of an apex predator at the edge of its range: impacts of changing sea ice on polar bears in Hudson Bay. *Ecol. Appl.* **26**, 1302–1320. (doi:10.1890/15-1256)

16. McGeachy D, Lunn NJ, Richardson ES, Derocher AE. 2025 Temporal dynamics of polar bear (*Ursus maritimus*) pregnancy rates in western Hudson Bay: influence of mass, age and timing of first breeding. *Conserv. Physiol.* **13**, coaf058. (doi:10.1093/conphys/coaf058)

17. Biddlecombe BA, Derocher AE, Krebs E, Lunn NJ, McGeachy D, Richardson ES. 2024 Building the foundation for polar bear science: Fifty years of research on polar bears in Western Hudson Bay. *Arct. Sci.* (doi:10.1139/as-2024-0056)

18. Regehr EV, Lunn NJ, Amstrup SC, Stirling I. 2007 Effects of earlier sea ice breakup on survival and population size of polar bears in Western Hudson Bay. *J. Wildl. Manag.* **71**, 2673–2683. (doi:10.2193/2006-180)

19. Clarke JC, Taylor RS, Manseau M. 2026 Runs of homozygosity predict inbreeding depression across taxa: a systematic review and meta-analysis. *Mol. Ecol.* **35**, e70541. (doi:10.1111/mec.70541)

20. Shafer ABA, Kardos M. 2025 Runs of homozygosity and inferences in wild populations. *Mol. Ecol.* **34**, e17641. (doi:10.1111/mec.17641)

21. Ceballos FC, Joshi PK, Clark DW, Ramsay M, Wilson JF. 2018 Runs of homozygosity: windows into population history and trait architecture. *Nat. Rev. Genet.* **19**, 220–234. (doi:10.1038/nrg.2017.109)

22. Fetterer F, Knowles K, Meier WN, Savoie M, Windnagel A, Stafford T. 2025 Sea Ice Index (G02135, Version 4). (doi:10.7265/A98X-0F50)

23. Meier WN, Stewart JS. 2023 NSIDC Land, Ocean, Coast, Ice, and Sea Ice Region Masks.

24. Jonkel C. 1967 Life history, ecology and biology of the polar bear, autumn 1966 studies. Canadian Wildlife Services.

25. Stirling I, Spencer C, Andriashek D. 1989 immobilization of polar bears (*Ursus maritimus*) with Telazol® in the Canadian Arctic. *J. Wildl. Dis.* **25**, 159–168. (doi:10.7589/0090-3558-25.2.159)

26. Calvert W, Ramsay MA. 1998 Evaluation of age determination of polar bears by counts of cementum growth layer groups. *Ursus* **10**, 449–453.

27. Derocher AE, Stirling I. 1995 Estimation of polar bear population size and survival in Western Hudson Bay. *J. Wildl. Manag.* **59**, 215–221. (doi:10.2307/3808933)

28. Lunn NJ, Stirling I, Andriashek D, Kolenosky GB. 1997 Re-Estimating the size of the polar bear population in Western Hudson Bay. *Arctic* **50**, 234–240.

29. Stapleton S, Atkinson S, Hedman D, Garshelis D. 2014 Revisiting Western Hudson Bay: Using aerial surveys to update polar bear abundance in a sentinel population. *Biol. Conserv.* **170**, 38–47. (doi:10.1016/j.biocon.2013.12.040)

30. Dyck M, Campbell M, Lee D, Boulanger J, Hedman D. 2016 2016 aerial survey of the Western Hudson Bay polar bear sub- population final report. 2017 Final Report. Government of Nunavut, Department of Environment, Wildlife Research Section, Status Report 2017-xx, Igloolik, NU.

31. Atkinson SN, Boulanger J, Campbell M, Trim V, Ware J, Roberto-Charron A. 2022 2021 aerial survey of the Western Hudson Bay polar bear subpopulation. 2022 Final Report. Government of Nunavut, Department of Environment, Wildlife Research Section, Status Report 2022-xx, Igloolik, NU.

32. Johnson AC, Reimer JR, Lunn NJ, Stirling I, McGeachy D, Derocher AE. 2020 Influence of sea ice dynamics on population energetics of Western Hudson Bay polar bears. *Conserv. Physiol.* **8**, coaa132. (doi:10.1093/conphys/coaa132)

33. Hostetter NJ, Lunn NJ, Richardson ES, Regehr EV, Converse SJ. 2021 Age-structured Jolly-Seber model expands inference and improves parameter estimation from capture-recapture data. *PLOS ONE* **16**, e0252748. (doi:10.1371/journal.pone.0252748)

34. Rohatgi A. 2024 WebPlotDigitizer V5. 2 URL: https://automeris.io. *WebPlotDigitizer2024*.

35. Drevon D, Fursa SR, Malcolm AL. 2017 Intercoder reliability and validity of WebPlotDigitizer in extracting graphed data. *Behav. Modif.* **41**, 323–339. (doi:10.1177/0145445516673998)

36. Ramsay MA, Stirling I. 1988 Reproductive biology and ecology of female polar bears (*Ursus maritimus*). *J. Zool.* **214**, 601–633. (doi:10.1111/j.1469-7998.1988.tb03762.x)

37. Derocher AE, Stirling I. 1996 Aspects of survival in juvenile polar bears. *Can. J. Zool.* **74**, 1246–1252. (doi:10.1139/z96-138)

38. McGeachy D, Lunn NJ, Derocher AE. 2024 Possible sexually selected infanticide by polar bears in western Hudson Bay. *Ursus* **2024**, 1–11. (doi:10.2192/URSUS-D-23-00028)

39. Richardson ES, Davis C, Stirling I, Derocher AE, Lunn NJ, Malenfant RM. 2020 Variance in lifetime reproductive success of male polar bears. *Behav. Ecol.* **31**, 1224–1232. (doi:10.1093/beheco/araa074)

554 40. Malenfant RM, Coltman DW, Davis CS. 2015 Design of a 9K illumina BeadChip for polar
555 bears (*Ursus maritimus*) from RAD and transcriptome sequencing. *Mol. Ecol. Resour.* **15**,
556 587–600. (doi:10.1111/1755-0998.12327)

557 41. Miller JM, Malenfant RM, Rivkin LR, Atwood TC, Baryluk S, Born EW, Dietz R, Laidre
558 KL, Pongracz J, Richardson ES, Wiig Ø, *et al.* 2024 Development of an 8K SNP chip to
559 assess adaptive diversity and hybridization in polar bears. *Conserv. Genet. Resour.*
560 (doi:10.1007/s12686-024-01359-1)

561 42. Rhodes E, Jerry D, Jones DB, Goldsbury J, Vu N. 2026 Swift SNPs: evaluating rapid DNA
562 extraction methods for scalable genotyping in aquaculture. *Mar. Biotechnol.* **28**, 15.
563 (doi:10.1007/s10126-025-10561-7)

564 43. Martin M. 2011 Cutadapt removes adapter sequences from high-throughput sequencing
565 reads. *EMBnet.journal* **17**, 10–12.

566 44. Li H, Durbin R. 2009 Fast and accurate short read alignment with Burrows–Wheeler
567 transform. *Bioinformatics* **25**, 1754–1760. (doi:10.1093/bioinformatics/btp324)

568 45. Li H *et al.* 2009 The Sequence Alignment/Map format and SAMtools. *Bioinformatics* **25**,
569 2078–2079. (doi:10.1093/bioinformatics/btp352)

570 46. Biscarini F, Cozzi P, Gaspa G, Marras G. 2019 Detect runs of homozygosity and runs of
571 heterozygosity in diploid genomes. R package version 0.9.6. Electronic file available at
572 https://CRAN.R-project.org/package=detectRUNS.

573 47. Chang CC, Chow CC, Tellier LCAM, Vattikuti S, Purcell SM, Lee JJ. 2015 Second-
574 generation PLINK: Rising to the challenge of larger and richer datasets. *GigaScience* **4**, 1–
575 16. (doi:10.1186/s13742-015-0047-8)

576 48. Liu S, Lorenzen ED, Fumagalli M, Li B Harris K, Xiong Z, Zhou L, Korneliussen TS, Somel
577 M, Babitt K, *et al.* 2014 Population genomics reveal recent speciation and rapid evolutionary
578 adaptation in polar bears. *Cell* **157**, 785–794. (doi:10.1016/j.cell.2014.03.054)

579 49. Meyermans R, Gorssen W, Buys N, Janssens S. 2020 How to study runs of homozygosity
580 using PLINK? A guide for analyzing medium density SNP data in livestock and pet species.
581 *BMC Genomics* **21**, 94. (doi:10.1186/s12864-020-6463-x)

582 50. Clendenin HR, Pollard MD, Puckett EE. 2025 Linking measures of inbreeding and genetic
583 load to demographic histories across three species of bears. *Evol. Appl.* **18**, e70133.
584 (doi:10.1111/eva.70133)

585 51. Purfield DC, Berry DP, McParland S, Bradley DG. 2012 Runs of homozygosity and
586 population history in cattle. *BMC Genet.* **13**, 70. (doi:10.1186/1471-2156-13-70)

587 52. Kardos M *et al.* 2018 Genomic consequences of intensive inbreeding in an isolated wolf
588 population. *Nat. Ecol. Evol.* **2**, 124–131. (doi:10.1038/s41559-017-0375-4)

53. Wiig Ø, Amstrup S, Atwood T, Laidre K, Lunn N, Obbard M, Regehr E, Thiemann G. 2015 *Ursus maritimus. The IUCN Red List of Threatened Species 2015*. (doi:10.2305/IUCN.UK.2015-4.RLTS.T22823A14871490.en)

54. Bürkner P-C. 2017 brms: An R package for bayesian multilevel models using Stan. *J. Stat. Softw.* **80**, 1–28. (doi:10.18637/jss.v080.i01)

55. Harrer M, Cuijpers P, Furukawa TA, Ebert DD. 2021 Bayesian Meta-Analysis. In *Doing Meta-Analysis with R*, Chapman and Hall/CRC.

56. Vehtari A, Gelman A, Gabry J. 2017 Practical Bayesian model evaluation using leave-one-out cross-validation and WAIC. *Stat. Comput.* **27**, 1413–1432. (doi:10.1007/s11222-016-9696-4)

57. McGeachy D. 2025 Influence of spatiotemporal dynamics of sea ice and individual effects on the population ecology of polar bears in Hudson Bay. Thesis Dissertation, University of Alberta. (doi:10.7939/83257)

58. Vongraven D, Derocher AE, Pilfold NW, Yoccoz NG. 2022 Polar bear harvest patterns across the circumpolar Arctic. *Front. Conserv. Sci.* **3**. (doi:10.3389/fcosc.2022.836544)

59. Lentfer J. 1974 Agreement on conservation of polar bears. *Polar Rec.* **17**, 327–330. (doi:10.1017/S0032247400032071)

60. Malenfant RM, Coltman DW, Richardson ES, Lunn NJ, Stirling I, Adamowicz E, Davis CS. 2016 Evidence of adoption, monozygotic twinning, and low inbreeding rates in a large genetic pedigree of polar bears. *Polar Biol.* **39**, 1455–1465. (doi:10.1007/s00300-015-1871-0)

61. Kardos M, Luikart G, Allendorf FW. 2015 Measuring individual inbreeding in the age of genomics: Marker-based measures are better than pedigrees. *Heredity* **115**, 63–72. (doi:10.1038/hdy.2015.17)

62. Zhang Q, Calus MP, Guldbrandtsen B, Lund MS, Sahana G. 2015 Estimation of inbreeding using pedigree, 50k SNP chip genotypes and full sequence data in three cattle breeds. *BMC Genet.* **16**, 88. (doi:10.1186/s12863-015-0227-7)

63. Knief U, Hemmrich-Stanisak G, Wittig M, Franke A, Griffith SC, Kempenaers B, Forstmeier W. 2015 Quantifying realized inbreeding in wild and captive animal populations. *Heredity* **114**, 397–403. (doi:10.1038/hdy.2014.116)

64. Taylor HR, Kardos MD, Ramstad KM, Allendorf FW. 2015 Valid estimates of individual inbreeding coefficients from marker-based pedigrees are not feasible in wild populations with low allelic diversity. *Conserv. Genet.* **16**, 901–913. (doi:10.1007/s10592-015-0709-1)

65. Mitchell C, Deakin S, Festa-Bianchet M, Pelletier F, Coltman D. 2026 No pedigree, no problem: genomic inbreeding tracks genetic rescue with high resolution. *Evol. Appl.* **19**, e70216. (doi:10.1111/eva.70216)

66. Hohenlohe PA, Funk WC, Rajora OP. 2021 Population genomics for wildlife conservation and management. *Mol. Ecol.* **30**, 62–82. (doi:10.1111/mec.15720)

67. Laidre KL, Atkinson SN, Regehr EV, Stern HL, Born EW, Wiig Ø, Lunn NJ, Dyck M, Heagerty P, Cohen BR. 2020 Transient benefits of climate change for a high-Arctic polar bear (*Ursus maritimus*) subpopulation. *Glob. Change Biol.* **26**, 6251–6265. (doi:10.1111/gcb.15286)

68. Aars J, Ieno EN, Andersen M, Derocher AE, Wiig Ø, Zuur AF. 2026 Body condition among Svalbard polar bears *Ursus maritimus* during a period of rapid loss of sea ice. *Sci. Rep.* **16**, 2182. (doi:10.1038/s41598-025-33227-9)

69. Crawford A, Stroeve J, Smith A, Jahn A. 2021 Arctic open-water periods are projected to lengthen dramatically by 2100. *Commun. Earth Environ.* **2**, 1–10. (doi:10.1038/s43247-021-00183-x)

70. Stroeve JC, Serreze MC, Holland MM, Kay JE, Malanik J, Barrett AP. 2012 The Arctic's rapidly shrinking sea ice cover: a research synthesis. *Clim. Change* **110**, 1005–1027. (doi:10.1007/s10584-011-0101-1)

71. Stroeve J, Notz D. 2018 Changing state of Arctic sea ice across all seasons. *Environ. Res. Lett.* **13**, 103001. (doi:10.1088/1748-9326/aade56)

72. Obbard ME, Cattet MRL, Howe EJ, Middel KR, Newton EJ, Kolenosky GB, Abraham KF, Greenwood CJ. 2016 Trends in body condition in polar bears (*Ursus maritimus*) from the Southern Hudson Bay subpopulation in relation to changes in sea ice. *Arct. Sci.* **2**, 15–32. (doi:10.1139/as-2015-0027)

73. Archer LC, Atkinson SN, Lunn NJ, Penk SR, Molnár PK. 2025 Energetic constraints drive the decline of a sentinel polar bear population. *Science* **387**, 516–521. (doi:10.1126/science.adp3752)

74. Andrews J, Babb D, Barber DG. 2018 Climate change and sea ice: Shipping in Hudson Bay, Hudson Strait, and Foxe Basin (1980–2016). *Elem. Sci. Anthr.* **6**, 19. (doi:10.1525/elementa.281)

75. Stroeve J, Crawford A, Ferguson S, Stirling I, Archer L, York G, Babb D, Mallett R. 2024 Ice-free period too long for Southern and Western Hudson Bay polar bear populations if global warming exceeds 1.6 to 2.6 °C. *Commun. Earth Environ.* **5**, 1–12. (doi:10.1038/s43247-024-01430-7)

76. Scott JBT, Marshall GJ. 2010 A step-change in the date of sea-ice breakup in Western Hudson Bay. *Arctic* **63**, 155–164.

77. Castro De La Guardia L, Myers P, Derocher A, Lunn N, Terwisscha Van Scheltinga A. 2017 Sea ice cycle in western Hudson Bay, Canada, from a polar bear perspective. *Mar. Ecol. Prog. Ser.* **564**, 225–233. (doi:10.3354/meps11964)

78. Derocher A, Stirling I. 1995 Temporal variation in reproduction and body mass of polar bears in western Hudson Bay. *Can. J. Zool.* **73**, 1657–1665. (doi:10.1139/z95-197)

79. Hobson KA, Stirling I, Andriashek DS. 2009 Isotopic homogeneity of breath CO_2 from fasting and berry-eating polar bears: implications for tracing reliance on terrestrial foods in a changing Arctic. *Can. J. Zool.* **87**, 50–55. (doi:10.1139/Z08-137)

80. Pagano AM, Rode KD, Lunn NJ, McGeachy D, Atkinson SN, Farley SD, Erlenbach JA, Robbins CT. 2024 Polar bear energetic and behavioral strategies on land with implications for surviving the ice-free period. *Nat. Commun.* **15**, 947. (doi:10.1038/s41467-023-44682-1)

81. Molnár PK, Bitz CM, Holland MM, Kay JE, Penk SR, Amstrup SC. 2020 Fasting season length sets temporal limits for global polar bear persistence. *Nat. Clim. Change* **10**, 732–738. (doi:10.1038/s41558-020-0818-9)

82. Northrup JM, Atkinson S, Howe E, Lunn NJ, Middel K, Obbard ME, Ross TR, Szor G, Walton L, Ware J. 2025 Estimating the abundance of a polar bear subpopulation at their southern global extent. *Can. J. Zool.* **103**, 1–14. (doi:10.1139/cjz-2024-0068)

83. McGeachy D, Lunn NJ, Northrup JM, Trim V, Davis C, Derocher AE. 2023 Distributional shifts of polar bears (*Ursus maritimus*) in Hudson Bay in relation to sea ice dynamics, 2017-2022 Final Report. Environment and Climate Change Canada.

84. Pollock KH, Nichols JD, Brownie C, Hines JE. 1990 Statistical inference for capture-recapture experiments. *Wildl. Monogr.* **107**, 3–97.

85. Wright S. 1931 Evolution in Mendelian Populations. *Genetics* **16**, 97–159. (doi:10.1093/genetics/16.2.97)

86. Mills LS, Allendorf FW. 1996 The one-migrant-per-generation rule in conservation and management. *Conserv. Biol.* **10**, 1509–1518. (doi:10.1046/j.1523-1739.1996.10061509.x)

87. Derocher AE, Stirling I. 1990 Distribution of polar bears (*Ursus maritimus*) during the ice-free period in western Hudson Bay. *Can. J. Zool.* **68**, 1395–1403. (doi:10.1139/z90-208)

88. Peacock E, Derocher AE, Lunn NJ, Obbard ME. 2010 Polar Bear Ecology and Management in Hudson Bay in the Face of Climate Change. In *A Little Less Arctic* (eds SH Ferguson, LL Loseto, ML Mallory), pp. 93–116. Dordrecht: Springer Netherlands. (doi:10.1007/978-90-481-9121-5_5)

89. Rivkin LR, Richardson ES, Miller JM, Atwood TC, Baryluk S, Born EW, Davis C, Dyck M, de Greef E, Laidre KL, Lunn NJ, *et al.* 2024 Assessing the risk of climate maladaptation for Canadian polar bears. *Ecol. Lett.* **27**, e14486. (doi:10.1111/ele.14486)